Design, Simulation, and Analog Circuit Implementation of a Three-Phase Shunt Active Filter Using the $\mathrm{I} \cos \Phi$ Algorithm

G. Bhuvaneswari, *Senior Member, IEEE*, and Manjula G. Nair

Abstract—A three-phase shunt active filtering algorithm based on the real component of fundamental load current ($\mathrm{I}\cos\phi$) has been proposed and implemented in a novel manner in this paper. The complete simulation and hardware implementation of the active filter (AF) with the proposed algorithm has been presented. Simulations have been performed for various dynamic operating conditions under balanced/unbalanced nonlinear reactive loads for both balanced as well as unbalanced/distorted source conditions. The AF has been realized by means of a hysteresis current-controlled voltage-source inverter (VSI). The experimental setup is controlled by making use of simple op-amp-based analog circuits and digital signal processor ADMC401. Experimental results have been obtained for different load and source conditions and discussed in detail. The response of the AF system in simulation as well as in hardware proves the effectiveness of the proposed control technique.

Index Terms—Analog and digital implementation, control algorithm, power quality (PQ), reactive nonlinear loads, shunt active filter (SAF).

I. INTRODUCTION

STATIC power converters, such as rectifiers, inverters, and other hard-switched power processing units are common sources of harmonic currents due to the switching action. The distorted current waveforms result in distorted voltages as well. The remedies for power-quality (PQ) problems are available in two forms: 1) passive filters and active filters for existing systems (retrofit) and 2) establishing new improved PQ converters. The discussion in this paper pertains to retrofit applications. Tuned passive filters are very effective for the elimination of specific harmonic components but are limited by drawbacks, such as fixed compensation, resonance, and huge size. Active filters [1], [2] overcome these drawbacks but are still limited by their rating and cost. Active filters are basically voltage-source or current-source inverters that provide the necessary compensation voltages/currents. A shunt active filter (SAF) generates a harmonic current spectrum that is opposite in phase to the harmonic and/or reactive current it perceives at the load end. Harmonic and reactive currents are thus cancelled at the
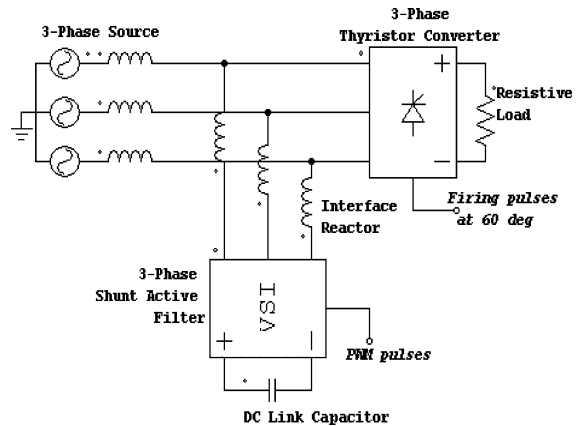
Fig. 1. Three-phase system with shunt AF.

source end and the result is undistorted sinusoidal balanced currents. The hybrid filters [3]–[5] combine passive and active filters, reducing the overall cost of the compensating circuit. The schematic diagram of an SAF installed in a three-phase system feeding a nonlinear load is depicted in Fig. 1.

II. CONTROL ALGORITHMS

The control algorithm for an SAF computes the reference compensation currents to be injected by the active filter (AF). The choice of the control algorithm therefore decides the accuracy and response time of the filter. The calculation steps involved in the control technique have to be minimal to make the control circuit compact. Instantaneous PQ theory [6], synchronous detection algorithm [7], dc-bus voltage algorithm [8], and synchronous reference frame theory [9] are some of the widely used three-phase shunt active filtering algorithms. There have been several research papers [10]–[14] on improving the aforementioned algorithms and hybrid filtering techniques, as these filters play an important role in solving many of the PQ problems in retrofit applications. The proposed $\mathrm{I}.\cos\phi$ control algorithm is one such simple scheme for achieving effective harmonic, reactive power and unbalance compensation. The authors had earlier proposed a simple current compensation algorithm for three-phase shunt active filters to provide only harmonic compensation [15]. In cases where both reactive power and harmonic compensation are provided, the source is supposed to supply only the active portion of the load current (i.e., $\mathrm{I}\cos\phi$, where "I" is the amplitude of the fundamental load current and $\cos\phi$ is the displacement power factor of the load).

So the proposed algorithm is named the "$\mathrm{I}\cos\phi$" algorithm. It is capable of providing 1) harmonic, 2) reactive power, and 3) unbalance compensation in conjunction with achieving unity power factor at the source end. The algorithm is designed to work successfully for balanced as well as unbalanced and distorted source voltages feeding balanced or unbalanced nonlinear reactive loads. In this paper, the concept of the proposed $\mathrm{I}.\cos\phi$ algorithm is described in detail. The simulation and hardware implementation of the three-phase shunt AF using the proposed control algorithm have been described subsequently. The results are compared with two conventional control schemes in simulation. In hardware, the reference compensation currents have been derived using op-amp-based analog circuits due to their simplicity. Further, ADMC 401 has been used to implement the hysteresis current controller to generate triggering signals for the devices in the AF. The digital hysteresis current controller allows the hysteresis band to be adjusted appropriately according to the requirement.

III. PROPOSED $\mathrm{I}.\cos\phi$ ALGORITHM

The shunt AF is expected to provide compensation for the harmonic and reactive portion of the three-phase load current, and for any imbalance in the three-phase load currents. This ensures that the balanced current will be drawn from the mains which will be purely sinusoidal and in phase with the mains voltage. So the mains is required to supply only the active portion of the load current. In the $\mathrm{I}.\cos\phi$ algorithm, the desired mains current is hence assumed to be the product of the magnitude $\mathrm{I}.\cos\phi$ and a unit amplitude sine wave in phase with the mains voltage.

Assuming a balanced source, the three-phase instantaneous voltages can be specified as

$$
\begin{aligned}
v_a &= V_m.\sin\omega t \\
v_b &= V_m.\sin(\omega t - 120°) \\
v_c &= V_m.\sin(\omega t + 120°).
\end{aligned}
\tag{1}
$$

Let this balanced three-phase source supply a nonlinear reactive load with some imbalance. For instance, let one of the phases of the load draw a lower current than the other two. The unbalanced, three-phase, reactive, harmonic-rich load currents can be expressed as

$$
\begin{aligned}
i_{La} &= I_{La1}.\sin(\omega t - \phi_a) + \sum_{n=2}^{\infty} I_{Lan}.\sin(n\omega t - \phi_{an}) \\
&= \mathrm{Re}.(i_{La1}) + \mathrm{Im}.(i_{La1}) + \text{harmonic\_components} \\
i_{Lb} &= I_{Lb1}.\sin(\omega t - 120° - \phi_b) \\
&\quad + \sum_{n=2}^{\infty} I_{Lbn}.\sin(n(\omega t - 120°) - \phi_{bn}) \\
&= \mathrm{Re}.(i_{Lb1}) + \mathrm{Im}.(i_{Lb1}) + \text{harmonic\_comps} \\
i_{Lc} &= I_{Lc1}.\sin(\omega t + 120° - \phi_c) \\
&\quad + \sum_{n=2}^{\infty} I_{Lcn}.\sin(n(\omega t + 120°) - \phi_{cn}) \\
&= \mathrm{Re}.(i_{Lc1}) + \mathrm{Im}.(i_{Lc1}) + \text{harmonic\_comps}
\end{aligned}
\tag{2}
$$

where

ϕ_a, ϕ_b, ϕ_c	phase angles of fundamental currents in a, b, and c phases;
$\phi_{an}, \phi_{bn}, \phi_{cn}$	phase angles of the nth harmonic currents in a, b, and c phases;
$I_{La1}, I_{Lb1}, I_{Lc1}$	three-phase fundamental current amplitudes;
$I_{Lan}, I_{Lbn}, I_{Lcn}$	three-phase nth harmonic current amplitudes.

The magnitude of the real component of the fundamental load current in each phase is given as

$$
\begin{aligned}
|\mathrm{Re}(I_{La1})| &= |I_{La}|.\cos\phi_a; \\
|\mathrm{Re}(I_{Lb1})| &= |I_{Lb}|.\cos\phi_b; \quad \text{and} \\
|\mathrm{Re}(I_{Lc1})| &= |I_{Lc}|.\cos\phi_c.
\end{aligned}
\tag{3}
$$

To ensure balanced, sinusoidal currents at a unity power factor to be drawn from the source, the magnitude of the desired source current can be expressed as the average of the magnitudes of the real components of the fundamental load currents in the three phases

$$
\begin{aligned}
\left|I_{s(\text{ref})}\right| &= \frac{|\mathrm{Re}(I_{La1})| + |\mathrm{Re}(I_{Lb1})| + |\mathrm{Re}(I_{Lc1})|}{3} \\
&= \frac{|I_{La}|.\cos\phi_a + |I_{Lb}|.\cos\phi_b + |I_{Lc}|.\cos\phi_c}{3}.
\end{aligned}
\tag{4}
$$

Let U_a, U_b, and U_c be the unit amplitude templates of the phase-to-ground source voltages in the three phases, respectively

$$
\begin{aligned}
U_a &= 1.\sin\omega t; \quad U_b = 1.\sin(\omega t - 120°); \\
\text{and} \quad U_c &= 1.\sin(\omega t + 120°).
\end{aligned}
\tag{5}
$$

The desired (reference) source currents in the three phases are therefore given as

$$
\begin{aligned}
i_{sa(\text{ref})} &= \left|I_{s(\text{ref})}\right| \times U_a = \left|I_{s(\text{ref})}\right|.\sin\omega t; \\
i_{sb(\text{ref})} &= \left|I_{s(\text{ref})}\right| \times U_b = \left|I_{s(\text{ref})}\right|.\sin(\omega t - 120°); \\
i_{sc(\text{ref})} &= \left|I_{s(\text{ref})}\right| \times U_c = \left|I_{s(\text{ref})}\right|.\sin(\omega t + 120°).
\end{aligned}
\tag{6}
$$

The reference compensation currents for the shunt AF are thereby deduced as the difference between the actual load current and the desired source current in each phase

$$
\begin{aligned}
i_{a(\text{comp})} &= i_{La} - i_{sa(\text{ref})}; \\
i_{b(\text{comp})} &= i_{Lb} - i_{sb(\text{ref})}; \quad \text{and} \\
i_{c(\text{comp})} &= i_{Lc} - i_{sc(\text{ref})}.
\end{aligned}
\tag{7}
$$

Equation (7) can be expanded as

$$
\begin{aligned}
i_{a(\text{comp})} &= [\mathrm{Re}.(i_{La1}) + \mathrm{Im}.(i_{La1}) + \text{harmonic\_components}] \\
&\quad - \left[\left|I_{s(\text{ref})}\right|.\sin\omega t\right] \\
i_{b(\text{comp})} &= [\mathrm{Re}.(i_{Lb1}) + \mathrm{Im}.(i_{Lb1}) + \text{harmonic\_components}] \\
&\quad - \left[\left|I_{s(\text{ref})}\right|.\sin(\omega t - 120°)\right] \\
i_{c(\text{comp})} &= [\mathrm{Re}.(i_{Lc1}) + \mathrm{Im}.(i_{Lc1}) + \text{harmonic\_components}] \\
&\quad - \left[\left|I_{s(\text{ref})}\right|.\sin(\omega t + 120°)\right].
\end{aligned}
\tag{8}
$$
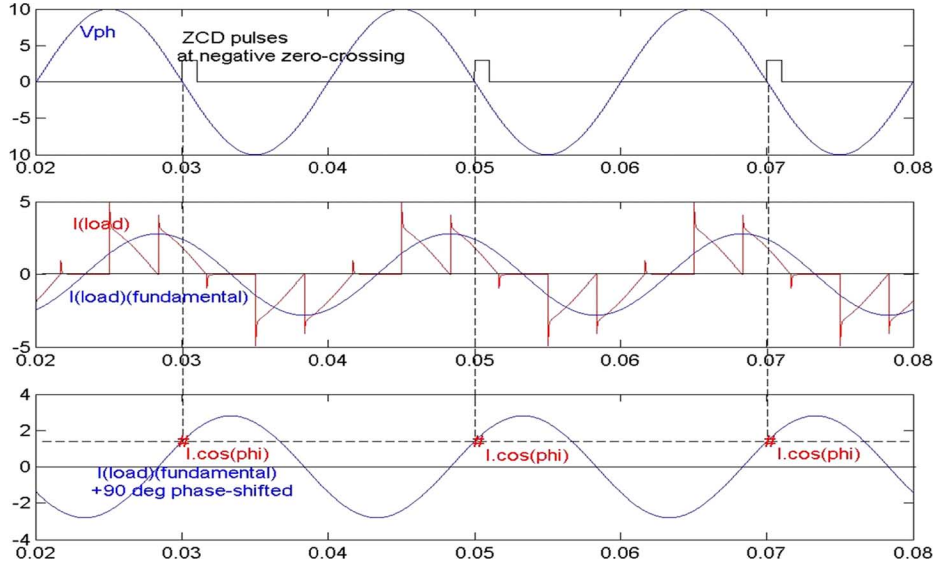
Fig. 2.   Illustration of the $\text{I.}\cos\phi$ algorithm.

If the three-phase load currents are balanced, then the reference compensation currents will essentially be the sum of the reactive component of load current and the harmonic components in each phase

$$i_{a(\text{comp})} = [\text{Im.}(i_{La1}) + \text{harmonic\_components}];$$
$$i_{b(\text{comp})} = [\text{Im.}(i_{Lb1}) + \text{harmonic\_components}];$$
$$i_{c(\text{comp})} = [\text{Im.}(i_{Lc1}) + \text{harmonic\_components}]. \quad (9)$$

The magnitude $\text{I.}\cos\phi$ is the active portion of the fundamental load current. This is extracted as the amplitude of the fundamental current, phase-shifted by $+90°$, at the negative going zero crossing of the phase voltage, as seen in Fig. 2. A second-order lowpass filter (which has 50 Hz as its cutoff frequency) is used to extract the fundamental load current with an inherent phase shift of $+90°$. This filter is actually a universal filter that has three portions that act as lowpass, highpass, and bandpass filters as explained in [16]. The lowpass filter is being used here. A zero crossing detector (ZCD) is used to detect the negative going zero crossing of the corresponding phase voltage. The fundamental component of the phase voltage is extracted using a lowpass filter before being fed to the ZCD to make it immune to any distortions in the incoming voltage. The ZCD has been designed with a tolerance of 5% to ensure that any oscillations around the zero-crossing are taken care of. The phase-shifted fundamental current goes as the "sample" input and the ZCD output pulse goes as the "hold" input to the "sample and hold" circuit whose output is the $\text{I.}\cos\phi$ magnitude. The average of these values in the three phases is then derived using a summing amplifier with a gain of 1/3. The block diagram of the control circuit for one of the three phases is given in Fig. 3. It clearly depicts how the reference compensation currents are generated by the op-amp-based control circuit.

The three-phase mains voltages are used as templates to generate unit amplitude sine waves in phase with mains voltages. In case the mains voltages are distorted, the fundamental com-

ponents of the mains voltages are extracted using second-order lowpass and used as the templates. The voltage fluctuations at the dc-bus capacitor of the AF are used to calculate the extra power loss in the inverter and the interface transformer. The corresponding phase current amplitude is calculated using a proportional integral and derivative (PID) controller [17] as follows and added to the active portion of the fundamental load current in each phase.

Assumption 1: The three-phase voltages V_{La}, V_{Lb} and V_{Lc} at the point of common coupling (PCC) are sinusoidal and balanced.

Assumption 2: The reference dc-link voltage is assumed to be $V_{\text{DC}}^{\star}$. The actual dc-link voltage is measured as V_{DC}.

Energy lost by the capacitor during the voltage discharge is

$$\Delta E = \frac{1}{2}C_{\text{DC}}\left(V_{\text{DC}}^{\star}{}^{2} - V_{\text{DC}}{}^{2}\right).$$

To keep V_{DC} constant, the energy drawn by the shunt AF from the ac mains must be equal to ΔE.

That is, Px T $= \Delta E$, where P $=$ active power drawn from AC mains $= 3/2.V_{Lm}.\text{I}_{\text{Cm}}$, where $V_{Lm} =$ magnitude of instantaneous phase voltage, V_{La}, V_{Lb}, or V_{Lc} and $I_{Cm} =$ magnitude of active current component, I_{Ca}, I_{Cb}, or I_{Cc} (corresponding to losses).

Therefore

$$I_{Cm} = \frac{C_{\text{DC}}\left(V_{\text{DC}}^{*}{}^{2} - V_{\text{DC}}{}^{2}\right)}{3.V_{Lm}.T} = \frac{C_{\text{DC}}\left(V_{\text{DC}}^{*}{}^{2} - V_{\text{DC}}{}^{2}\right)\omega}{6.\pi.V_{Lm}} \quad (10)$$

where T $= 2.\pi/\omega$ and ω is the sampling frequency.

This loss component is added to the magnitude of the reference compensation current in each phase. This ensures that the losses in the AF are being taken care of by the three-phase source and the dc-bus voltage of the AF becomes a self-supporting one.

The reference compensation currents for the shunt AF are thereafter computed as the difference between the actual load currents and the desired mains currents for the three phases.
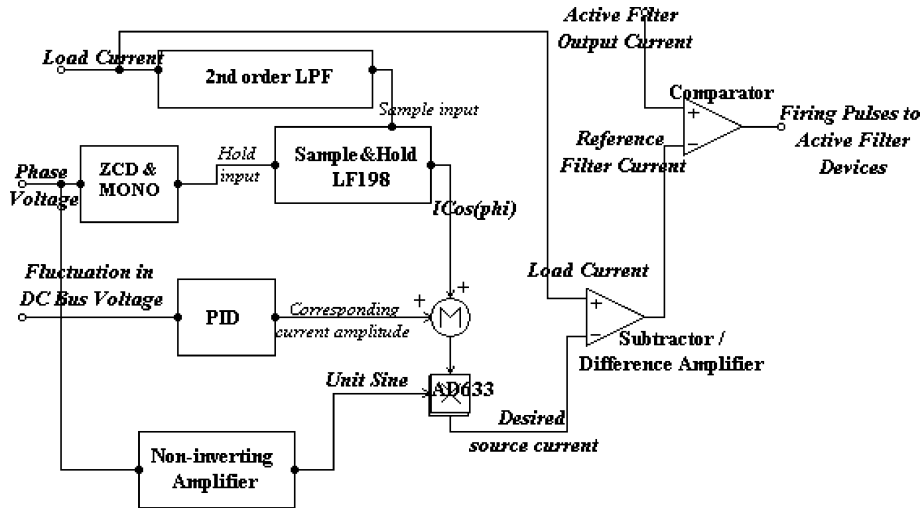
Fig. 3. Block diagram of the op-amp-based control circuit.
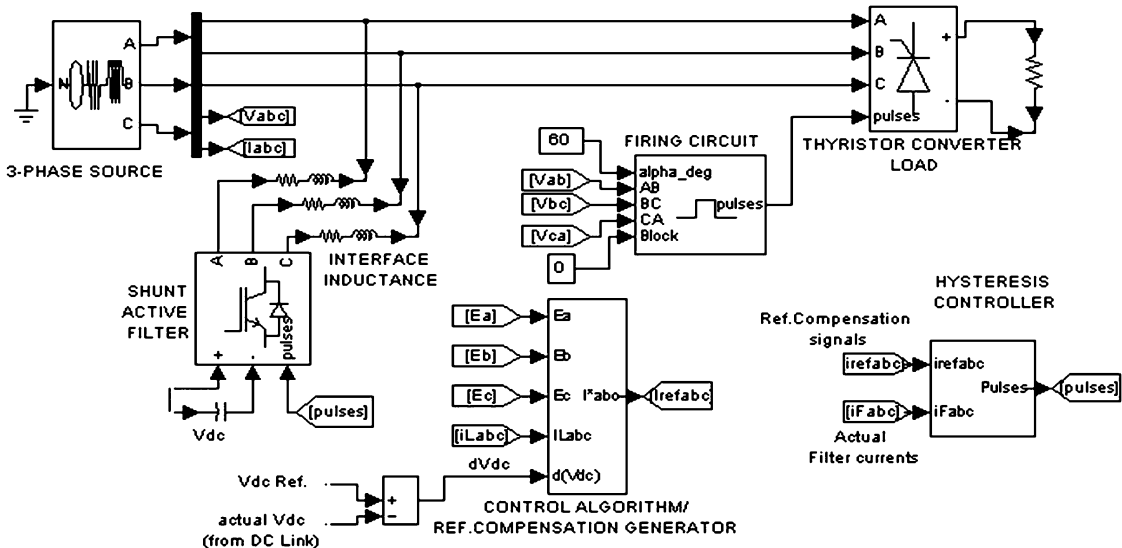
Fig. 4. Simulation model of the three-phase system with a shunt AF.

IV. SIMULATION OF THE SHUNT ACTIVE FILTER

The system considered for simulation is a three-phase balanced source supplying a thyristorized bridge rectifier feeding a resistive load, operating at a triggering angle of 60°, as shown in Fig. 4. This load draws a highly nonlinear current rich in harmonics with a substantial reactive power requirement. A three-phase, VSI-based shunt AF is connected to the system for reactive power compensation and harmonics elimination.

The simulation is performed in the Simulink/MATLAB environment. The system parameters are phase voltage $= 230$ V and dc side $R = 150\ \Omega$. The interface reactor used is 1.5 mH and the dc-link capacitor is 5000 μF with the dc-link reference voltage being 650 V.

V. HARDWARE IMPLEMENTATION

The three-phase shunt active filtering algorithm has been implemented in hardware using analog circuits and an ADMC-401

digital signal processor as mentioned earlier. The three-phase load for which the compensation is to be provided is a thyristor-controlled converter feeding a resistive load. The triggering angle (α) of the converter is adjusted to 60° so that the converter draws highly nonlinear reactive currents. A three-phase voltage-source inverter with a suitable dc-link capacitor having a self- supporting dc-bus voltage and an interfacing three-phase reactor is made to act as the SAF to generate compensation currents.

The compensation currents are generated using a simple control circuit made up of six operational amplifiers, a sample-and-hold circuit and an analog multiplier as described in Section III. The various components of this circuit are the biquad filter (a second-order lowpass filter made up of three op-amps), sample-and-hold circuit LF198, negative-going zero crossing detector (ZCD) and monostable multivibrator, a summing amplifier with a gain of 1/3, a noninverting amplifier (with an appropriate gain to derive unit amplitude sine-wave templates from three-phase
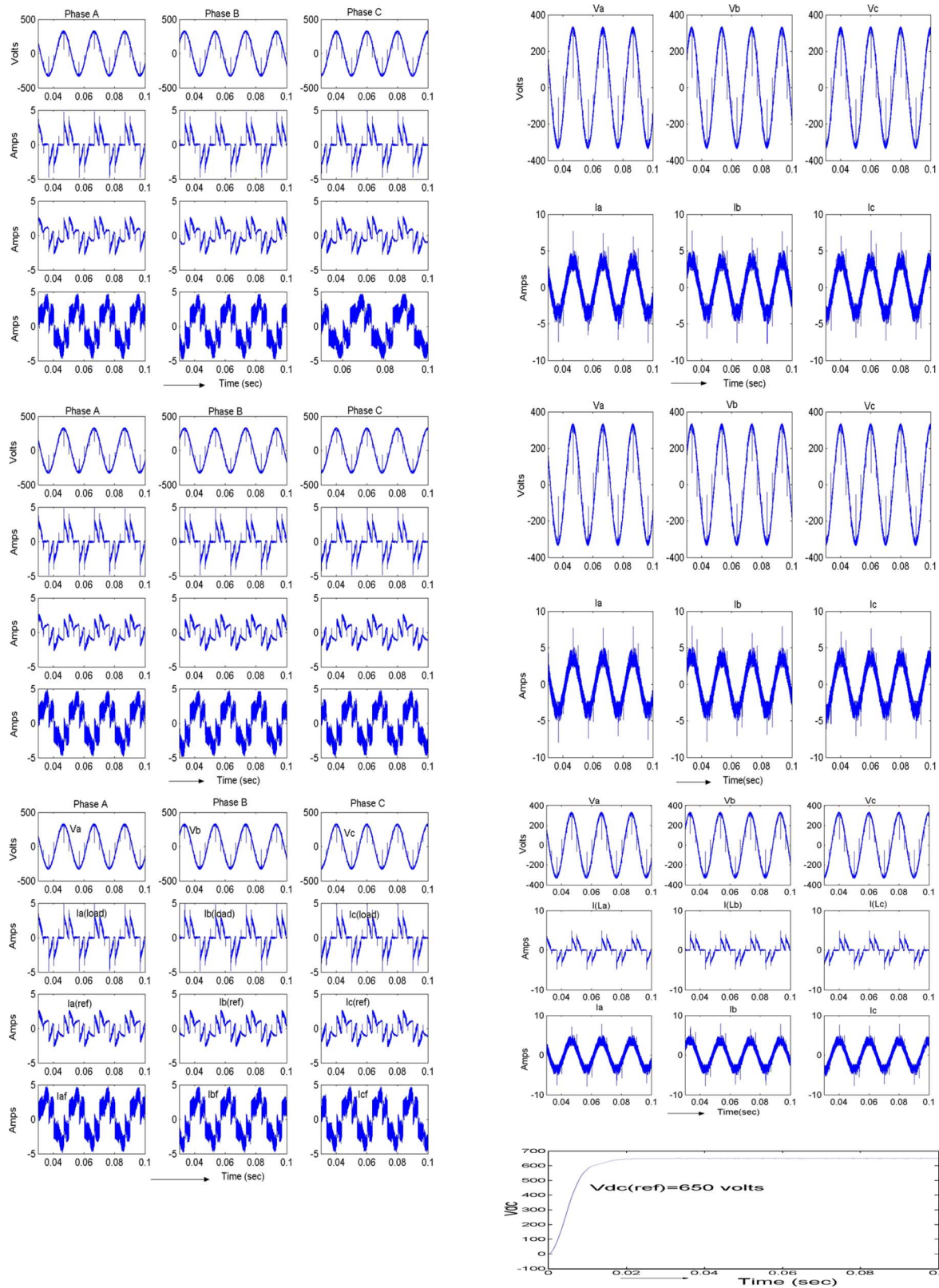
Fig. 5. Simulation results under balanced source-balanced load. 1) instantaneous PQ theory, 2) synchronous detection algorithm, 3) $\text{I.}\cos\phi$ algorithm source voltage, load current, reference filter current, actual filter current (on the left side), source voltage and current after compensation, and dc-link voltage (on the right side).

mains voltages), and an analog multiplier AD633 (to calculate the magnitude of the desired source current as the product of the average amplitude $\text{I.}\cos\phi$ and the unit sine wave). A discrete PID controller is used to calculate the current amplitude corre-
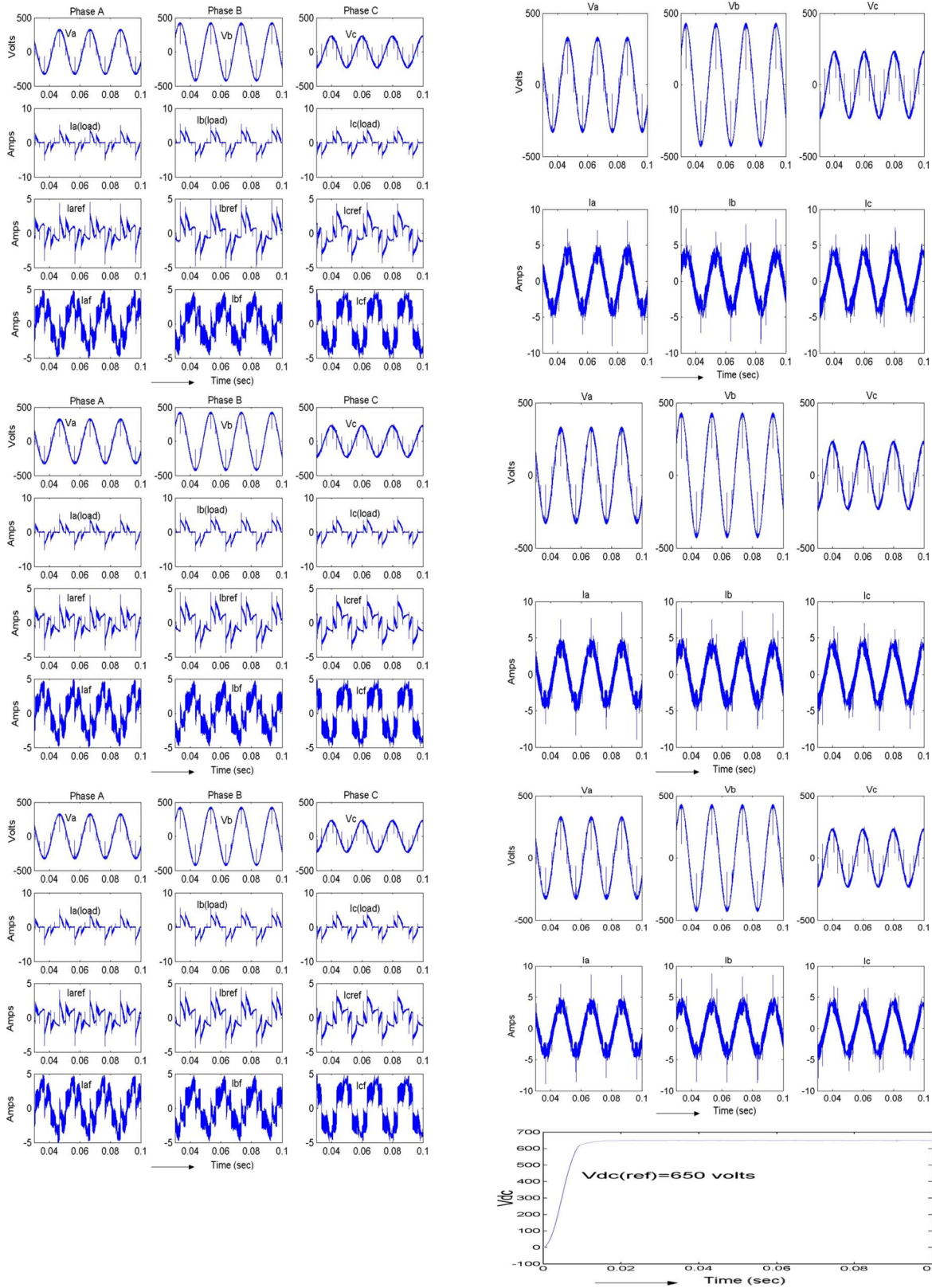
Fig. 6. Simulation results under unbalanced source-balanced load. 1) instantaneous PQ theory; 2) synchronous detection algorithm; 3) $I.\cos\phi$ algorithm source voltage, load current, reference compensation current, and filter output current (on the left side) source voltage and source current after compensation and dc-link capacitor voltage, Vdc (on the right side).

sponding to losses in an inverter. To start with, the proportional gain K_p is arrived at based on (10). The controller parameters have further been tuned on a trial-and-error basis to arrive at $K_p = 2$, $K_i = 0.5$, and $K_d = 0$.
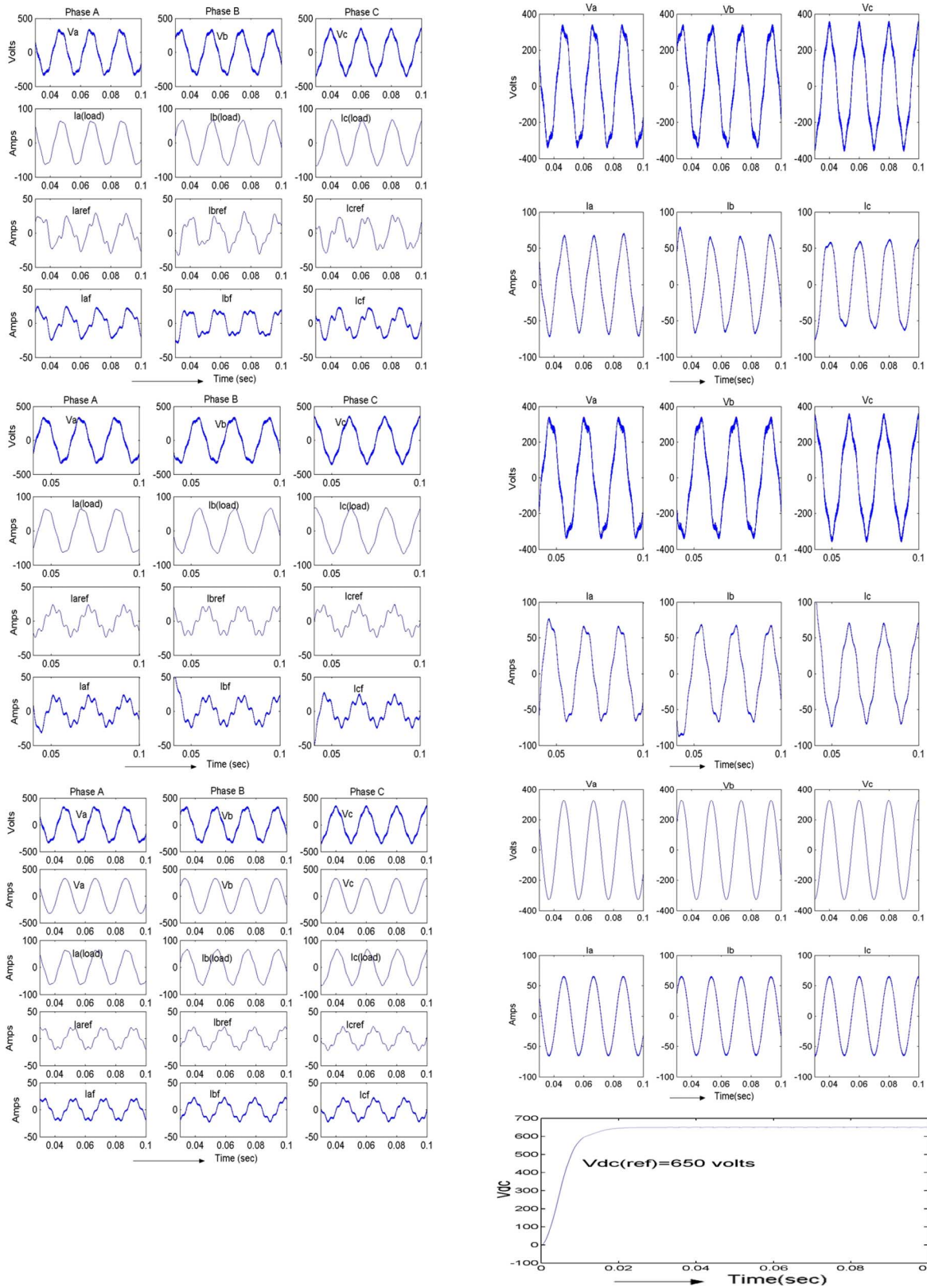
Fig. 7.   Simulation results under distorted source-balanced load. 1) instantaneous PQ theory; 2) synchronous detection algorithm; 3) $I.\cos\phi$ algorithm distorted phase voltage, sinusoidal phase voltage, load current, reference compensation current, and filter output current (on the left side) phase voltage, source current after compensation and dc-link capacitor voltage, Vdc (on the right side).

A hysteresis comparator routine developed in the digital signal processor (DSP) ADMC401 is used to generate the required triggering pulses to the devices in the filter. The reference compensation currents generated using analog cir-
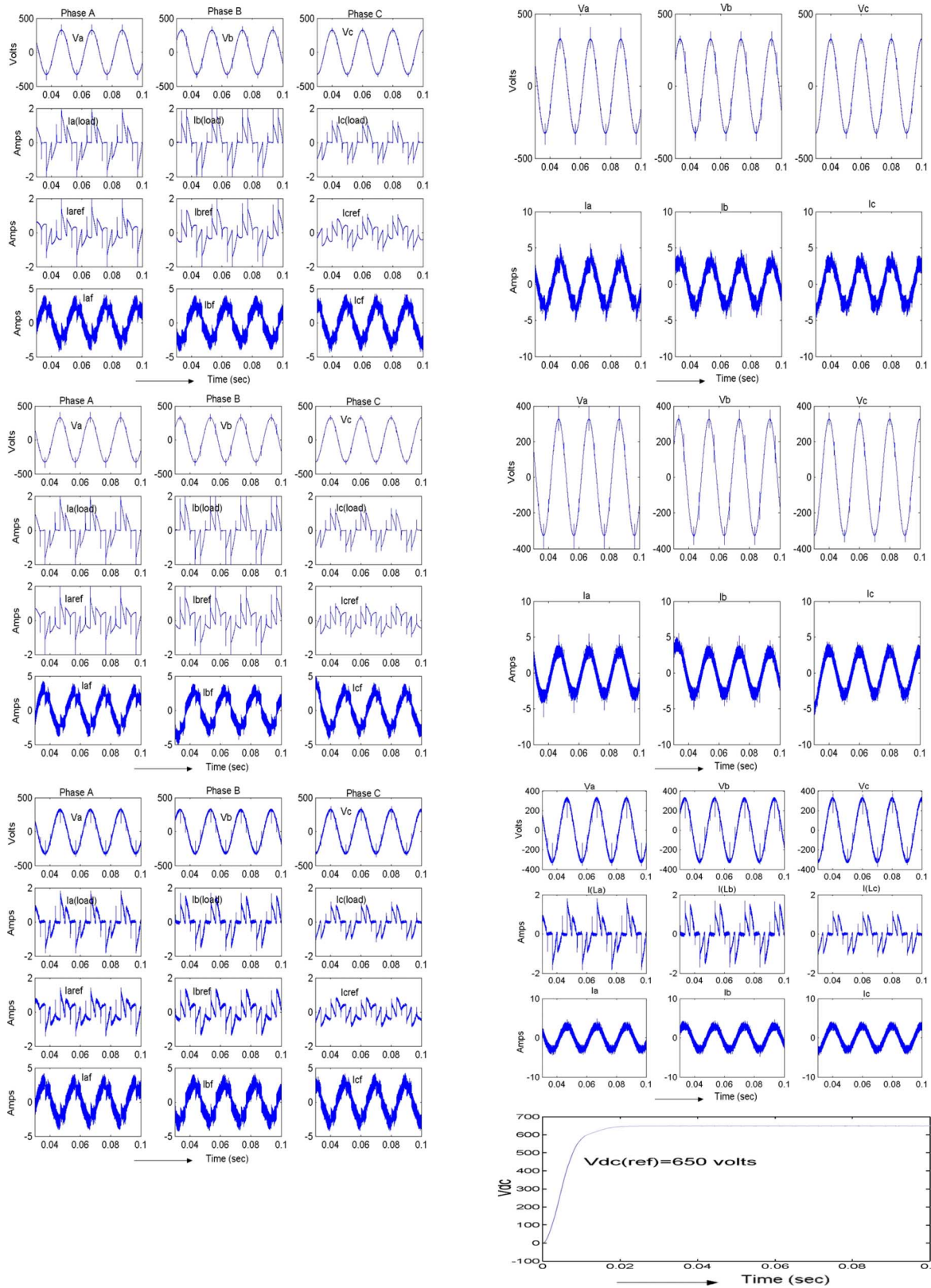
Fig. 8. Simulation results under balanced source-unbalanced load: 1) instantaneous PQ theory, 2) synchronous detection algorithm, 3) $I.\cos\phi$ algorithm phase voltage, load current, reference compensation current, and filter output current (on the left side). Phase voltage, source current after compensation, and dc-link capacitor voltage, Vdc (on the right side).

cuits and the actual output currents of the SAF sensed using Hall-effect current sensors are fed to the analog-to-digital

converter (ADC) ports of the DSP. The comparator routine compares the two signals for each phase and generates trig-
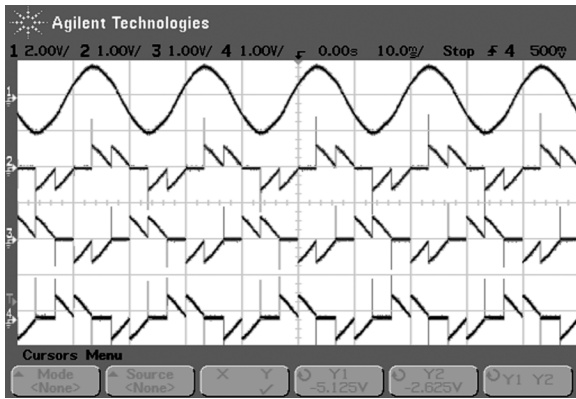
Fig. 9. Three-phase currents for a thyristor converter at $\alpha = 60°$ (a) source voltage in a-phase (b) load currents in a-phase (c) in b-phase (d) in c-phase.

(a)
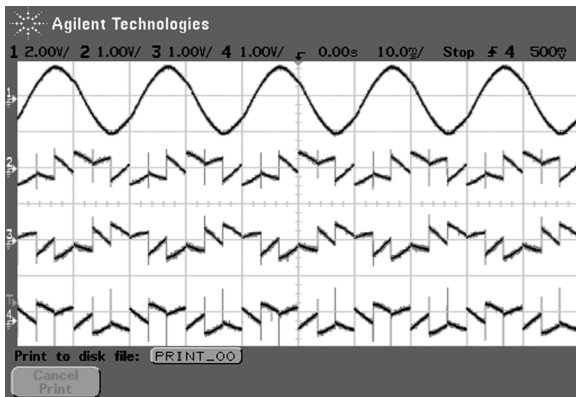
Fig. 10. Compensation currents. (a) Source voltage in a-phase (b), compensation current in a-phase, (c) in b-phase (d), and in c-phase.

(b)

gering pulses depending on the sampling rate and hysteresis band. The hysteresis comparator has been implemented in the DSP to facilitate appropriate adjustment of the hysteresis band according to the requirement of the system. The sampling frequency adopted is 10 kHz which ensures the elimination of harmonics up to the 100th order. A driver circuit comprised of optocouplers and amplifiers boosts the output pulses from the DSP to the required voltage levels of the inverter devices. The optocouplers isolate the control circuit from the power circuit for preventing the interferences that could affect the functioning of the control circuitry.

VI. RESULTS AND DISCUSSION

The results obtained from the simulation and experimental setup are presented in this section. The simulations are performed for two conventional control algorithms as well, namely, instantaneous PQ theory and a synchronous detection algorithm for the purpose of comparison with the proposed algorithm. For the ideal case where the source voltages as well as the loads in the three phases are balanced, the actual compensation currents generated by the shunt AF for the three phases are found to follow the respective reference
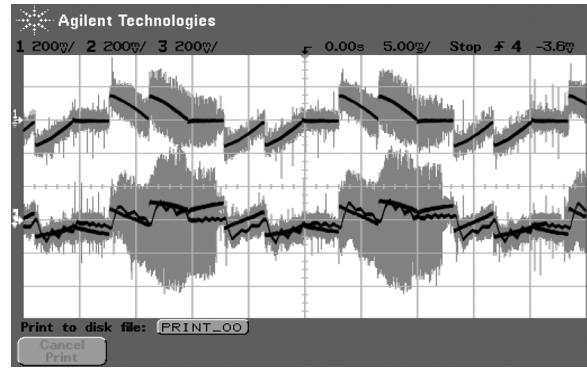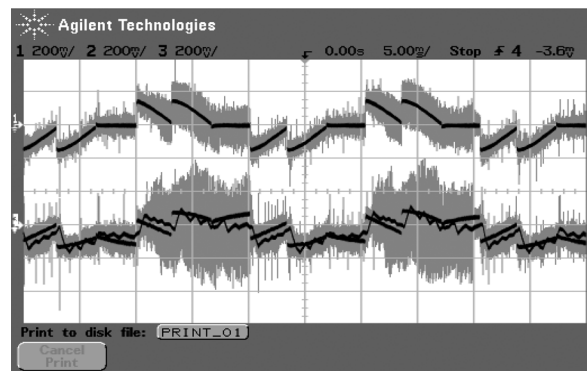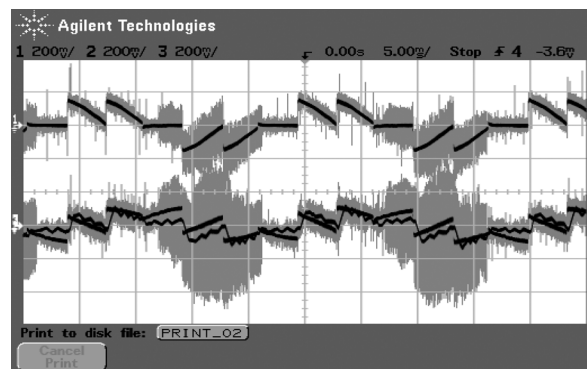
(c)

Fig. 11. (a) Reference compensation signals and the actual AF currents for a-phase: 1) load current and 2) reference and actual compensation currents (superimposed) A. (b) Reference compensation signals and the actual AF currents for b-phase: 1) load current and 2) reference and actual compensation currents (superimposed) A. (c) Reference compensation signals and the actual AF currents for c-phase: 1) load current and 2) reference and actual compensation currents (superimposed) A.

compensation currents exactly in simulation as given in Fig. 5 [18]. This is true for all three algorithms. The corresponding experimental results are given in Figs. 9–11, respectively.
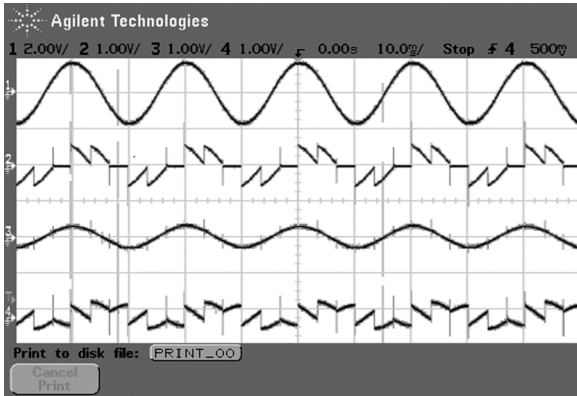
Fig. 12. Waveforms for the AF in a-phase. (a) Source voltage. (b) Load current. (c) Desired source current. (d) Reference compensation current.
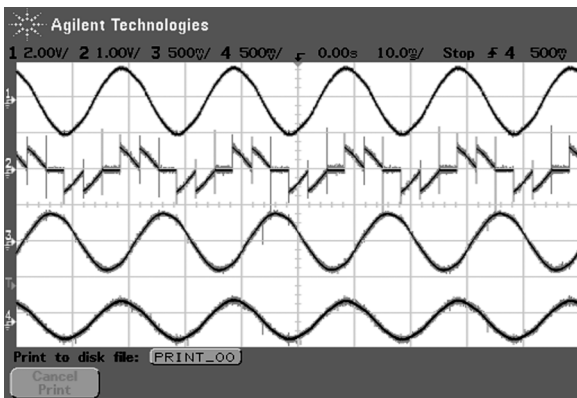
Fig. 13. Waveforms of a-phase voltage and current signals. (a) Source voltage. (b) Load current. (c) Fundamental component of load current with $+90°$ phase-shift. (d) Desired source current.

The three-phase balanced supply of 400 V is applied to the fully controlled thyristor converter drawing a current of about 7 A. The controlled rectifier operates at a triggering angle of $60°$ so that the load currents drawn are at a power factor that is much less than unity as shown in Fig. 9. The compensation currents generated by the $I.\cos\phi$ algorithm for all of the three phases are shown in Fig. 10. The filter output currents shown in Fig. 11 are found to match exactly with the reference compensation currents in all three phases. The desired source current takes care of only the real power requirement of the load, losses in the AF and the interphase reactor, and has a unity power factor as shown in Fig. 12. The reference compensation current provides harmonic as well as reactive power compensation as seen from Figs. 10 and 12. The fundamental component of the load current extracted from the second-order LPF contains the reactive component also. However, the desired source current after compensation supplies only the active portion of the load current. This difference is visible from the corresponding plots shown in Fig. 13 for the a-phase.

The effectiveness of the $I.\cos\phi$ control algorithm is evident from the simulation results depicted in Fig. 5. The source currents in all three phases are pure sinusoids with a unity power factor. The corresponding experimental results are shown in Fig. 14. The source currents are found to be fairly sinusoidal, in phase with the respective voltages (unity power factor), as expected. Fig. 14(d) and (e) shows the harmonic spectrum of the source current before and after compensation which shows the effectiveness of the functioning of the AF.

The $I.\cos\phi$ control algorithm is found to work satisfactorily under unbalanced and/or distorted source voltage conditions and also for unbalanced load conditions. This can be seen from the simulation results obtained for the aforementioned operating conditions, with the three control algorithms. Under unbalanced source voltage conditions, a 30% amplitude unbalance is introduced in the b and c phases so that the phase voltages are 230 V in phase a, 300 V in phase b, and 160 V in phase c, respectively. The unbalance is reflected on the load currents in the three phases too. However, the AF takes care of the source currents to make them balanced. Fig. 6 shows the response of the system for unbalanced source conditions for all three control algorithms. It is seen from the results that all three control algorithms give satisfactory results under unbalanced source voltages.

When there is distortion in the supply voltages, the fundamental components of the distorted source voltages are extracted using second-order lowpass filters whose cutoff frequency is 50 Hz. The second-order lowpass filter realized in analog circuit gives outputs almost instantaneously. Then, the compensation currents are generated using the $I.\cos\phi$ algorithm. Fig. 7 shows the simulation results for distorted source voltage conditions. The distorted voltages are applied to a balanced linear load, which is a series RL load. A fifth harmonic voltage of 10% of the fundamental added to the normal 50-Hz sinusoidal supply voltage gives the distorted voltage in each phase. The conventional controllers give poor results compared to the proposed controller. Figs. 15 and 16 show the distorted voltages in the three phases and how the voltages are filtered and balanced source voltages are generated experimentally.

When an unbalanced nonlinear load is connected to a balanced source, load currents in the three phases reflect the unbalance. The source is, however, expected to supply balanced three-phase currents, with the rest of the unbalanced portion of the currents in the corresponding phases being supplied by the SAF along with the harmonic and reactive power components. In the $I.\cos\phi$ control scheme, the magnitudes of the active portions of the fundamental load currents in the three phases $|I_a.\cos\phi_a|$, $|I_b.\cos\phi_b|$ and $|I_c.\cos\phi_c|$ are detected using the sample–and-hold circuit LF198 for each phase.

The average of these magnitudes is computed using a summing amplifier circuit with a proper gain and fed to the analog multiplier AD633 chips in the three phases to be multiplied with the unit amplitude sine waves. This makes sure that the magnitudes of the desired source currents in all three phases
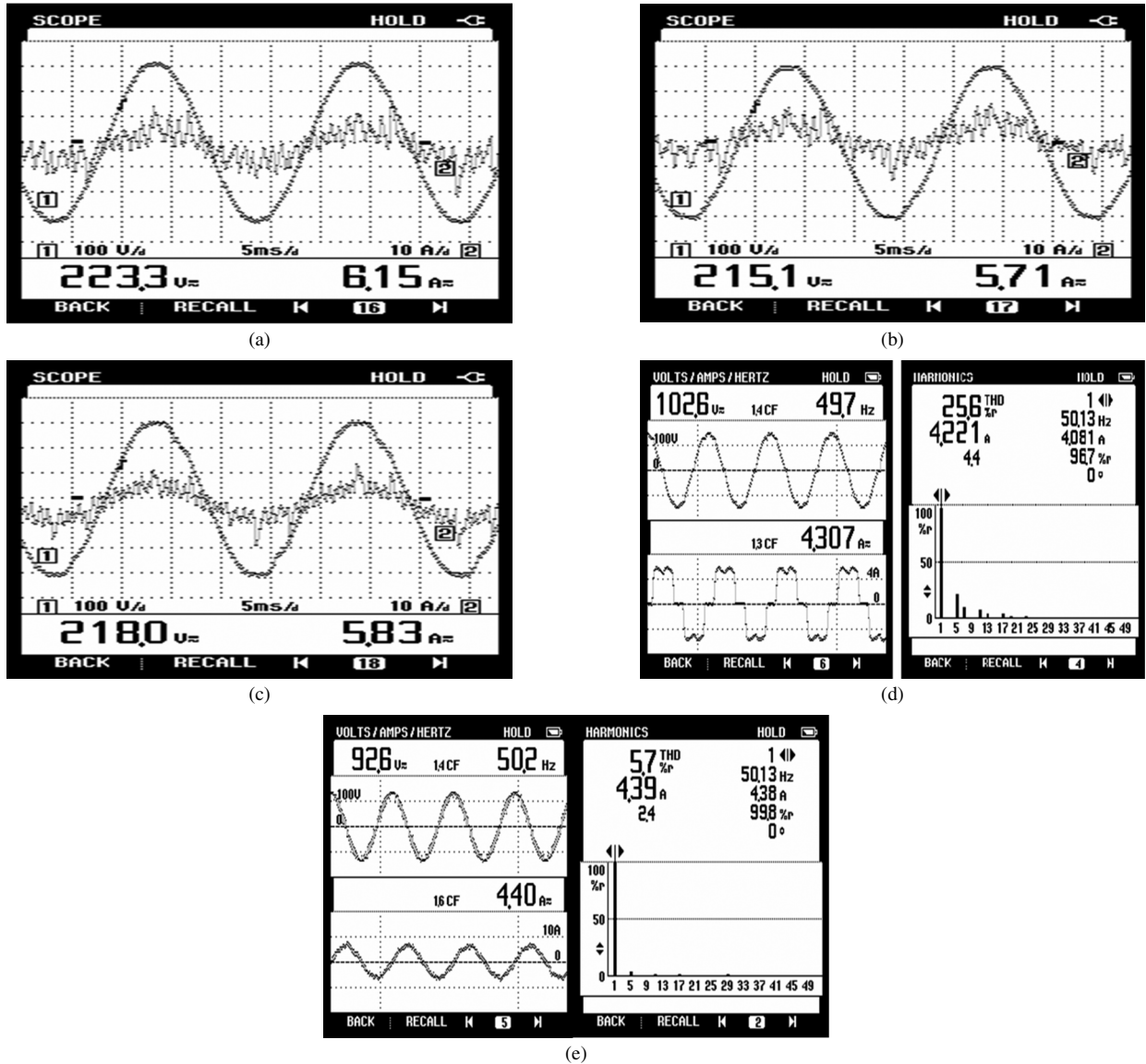
Fig. 14. (a) Source voltages and currents for a-phase after compensation: 1) phase voltage and 2) sinusoidal source current at unity power factor. (b) Source voltages and currents for b-phase after compensation: 1) phase voltage and 2) sinusoidal source current at unity power factor. (c) Source voltages and currents for c-phase after compensation: 1) phase voltage and 2) sinusoidal source current at unity power factor. (d) Line voltage V_{AB} and C phase load current and its harmonic spectrum for a diode rectifier load before compensation at 100 V. (e) Voltage V_{AB} and C phase source current and its harmonic spectrum for a diode rectifier load after compensation at 100 V.
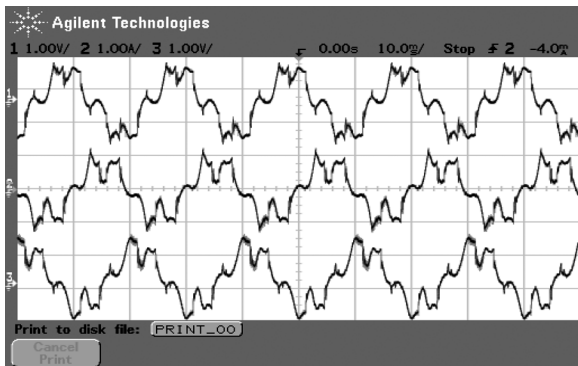
Fig. 15. Experimental results for the distorted/unbalanced source voltage condition—three-phase distorted/unbalanced source voltages.

remain the same even in case of load unbalance. Fig. 8 shows the simulation results under the unbalanced load conditions for

all the three control schemes. The corresponding experimental results for the $I. \cos \phi$ control scheme are given in Figs. 17–19. Table I lists the %THD of the mains current before and after shunt compensation based on the three control schemes, in simulation. The %THD is found to be within the limits of 5% as expected by IEEE standards, under all operating conditions only with the $I. \cos \phi$ control scheme. The dc-link capacitor voltage V_{DC} of the AF settles at 650 V (reference value) in all cases.

To prove the effectiveness of the $I. \cos \phi$ algorithm, the dynamic response of the filter has also been tested by introducing load variation. Figs. 20 and 21 show the simulation and experimental results for the starting response time of the AF, which is about 6.8 ms (i.e., approximately one-third of a cycle. Figs. 22 and 23 illustrate the response of the control circuit and the filter for a sudden increase in load. The response time is less than
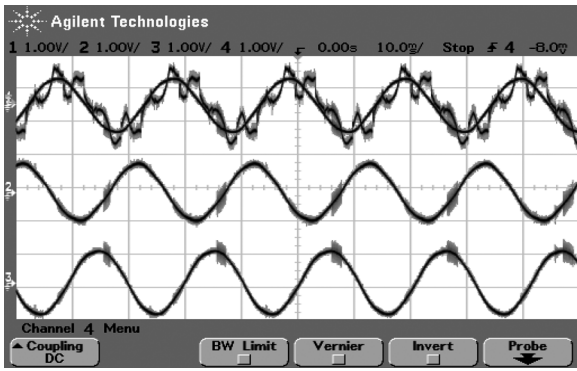
(a)
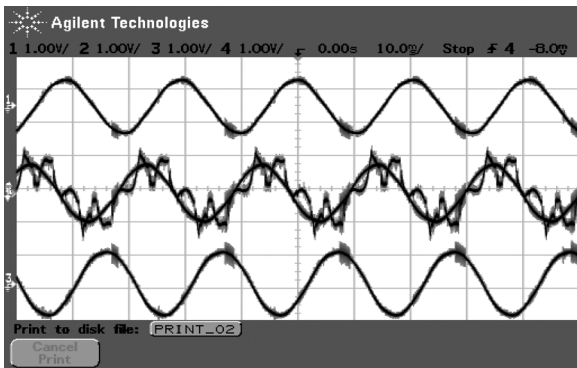
(b)
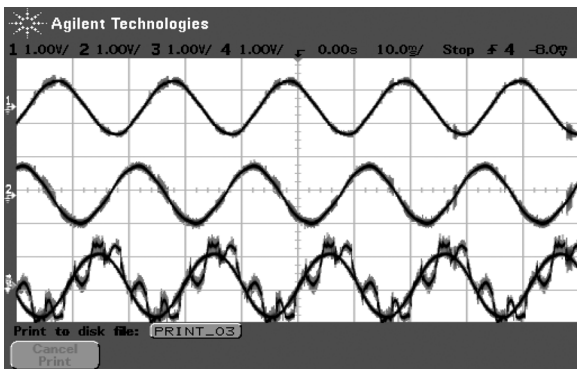
(c)

Fig. 16. (a) Experimental results for the distorted/unbalanced source voltage condition—distorted source voltage of a-phase and three-phase sinusoidal voltages after filtering. (b) Distorted source voltage of b-phase and three-phase sinusoidal voltages after filtering. (c) Distorted source voltage of c-phase and three-phase sinusoidal voltages after filtering.

Fig. 17. Experimental results for load unbalance condition—three-phase unbalanced load currents.
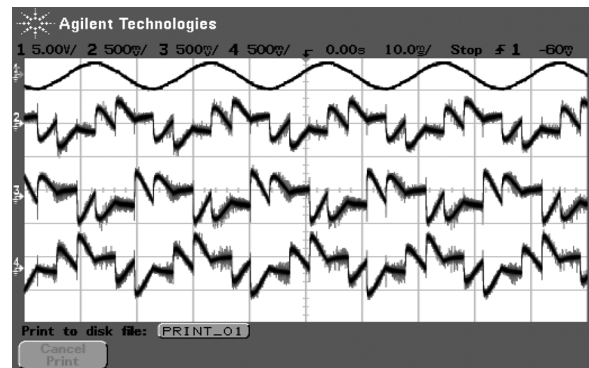
Fig. 18. Experimental results for load unbalance condition—three-phase compensation currents.
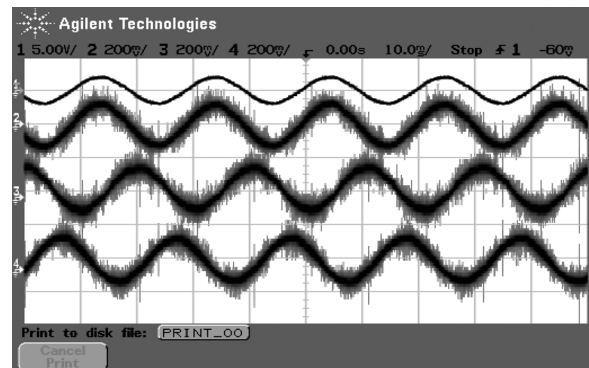
Fig. 19. Experimental results for load unbalance condition—desired source currents in the three phases.

100 μs. The dc-link capacitor voltage V_{DC} of the AF is also seen (Fig. 22) to settle after small disturbances near the transient point ($t = 0.06$ s), at the reference voltage of 650 V even under load perturbations. This proves that the AF functions very well under dynamic operating conditions.

VII. CONCLUSION

This paper proposes the I. $\cos\phi$ algorithm for SAF based on the active portion of the fundamental load current. A simple, efficient, and novel way of implementing this algorithm by making use of some op-amp circuits and a digital signal processor ADMC401 has also been proposed here. The simplicity and ruggedness of the algorithm is evident from its easy analog circuit implementation and its response in a three-phase system drawing nonlinear reactive balanced/unbalanced currents. The algorithm is applicable in all operating

TABLE I
%THD IN THE MAINS CURRENTS AFTER COMPENSATION

METHOD USED	%THD balanced source/ balanced load	%THD unbalanced source/ balanced load	%THD balanced source/ unbalanced load
Before compensation	58.95%	81.99%	66.46%
IRPT	5.1%	7.12%	4.07%
SD	3.7%	6.19%	7.62%
I.cosϕ	3.77%	4.46%	3.05%

Fig. 22. Response to load transient—simulation results. (a) Phase voltage. (b) Load current. (c) Reference compensation current. (d) Actual filter current. (e) DC-link capacitor voltage (Vdc). (f) Vdc expanded near load transient (t = 0.06 s).
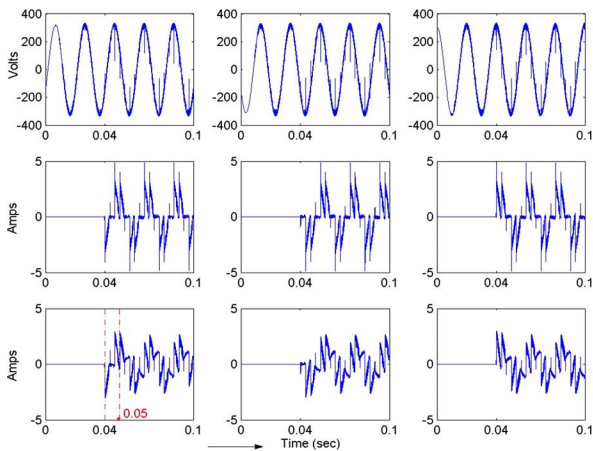
Fig. 20. Starting response—simulation results: 1) phase voltage (V), 2) load current, 3) desired source current, 4) reference filter current (A).
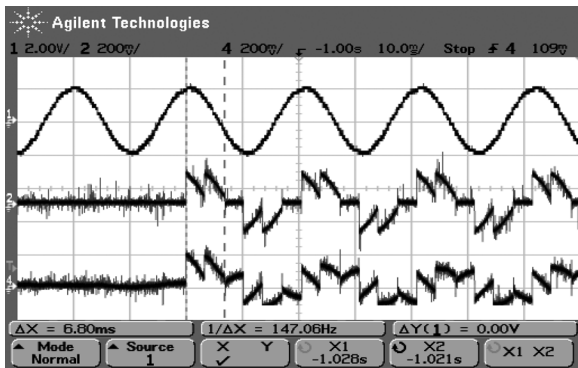
Fig. 21. Starting response time = 6.8 ms—experimental results: 1) phase voltage (V), 2) load current, and 3) reference filter current (A).
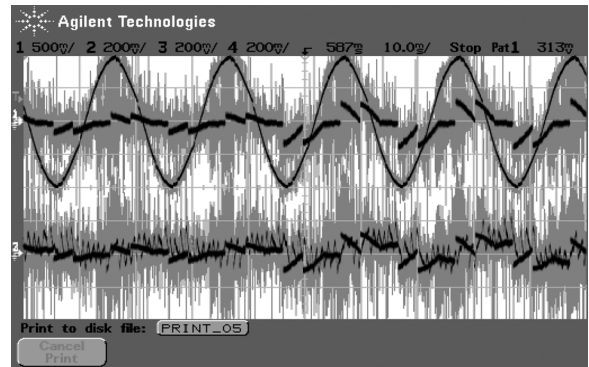
Fig. 23. Response to load transient—experimental results: 1) phase voltage, V and load current (A) and 2) reference and actual filter currents (A).

conditions of the three-phase system, such as balanced, unbalanced, and distorted source voltages and nonreactive as well as reactive, balanced/unbalanced, and nonlinear loads. The results presented here prove the effectiveness of the algorithm under all operating conditions. The algorithm is found to work satisfactorily during starting conditions and load perturbations. In all, this paper presents a simple and effective control algorithm for SAFs for providing current compensation in a three-phase balanced/unbalanced system feeding nonlinear reactive loads.

REFERENCES

[1] S. Rahmani, K. Al-Haddad, and F. Fnaiech, "A three-phase shunt active power filter for damping of harmonic propagation in power distribution networks," in *Proc. IEEE Int. Symp. Industrial Electronics*, Jul. 2006, vol. 3, pp. 1760–1764.

[2] X. Wang, J. Liu, C. Yuan, and Z. Wang, "Generalized control approach for active power filters," in *Proc. IEEE Int. Conf. Power Electronics Motion Control*, Aug. 2006, vol. 1, pp. 1–5.

[3] M. Rastogi, N. Mohan, and A. A. Edris, "Filtering of harmonics currents and damping of resonances in power systems with a hybrid active filter," in *Proc. IEEE Applied Power Electronics Conf.*, Dallas, TX, 1995, pp. 607–612.

[4] B.-R. Lin *et al.*, "Analysis and operation of hybrid active filter for harmonic elimination," *Elect. Power Syst. Res.*, vol. 62, pp. 191–200, 2002.

[5] S. Kim and P. N. Enjeti, "A new hybrid active power filter (APF) topology," *IEEE Trans. Power Electron.*, vol. 17, no. 1, pp. 48–54, Jan. 2002.

[6] J. H. Akagi, Y. Kanazawa, and A. Nabae, "Instantaneous reactive power compensators comprising switching devices without energy storage components," *IEEE Trans. Ind. Appl.*, vol. IA-20, no. 3, pp. 625–630, May/Jun. 1984.

[7] C. L. Chen, C. E. Lin, and C. L. Huang, "Reactive and harmonic current compensation for unbalanced three-phase systems using the synchronous detection method," *Elect. Power Syst. Res.*, vol. 26, pp. 163–170, 1993.

[8] H. L. Jou, "Performance comparison of the three-phase-active-power-filter algorithms," in *Proc. Inst. Elect. Eng., Gen., Transm. Distrib.*, 1995, pp. 646–652.

[9] S. Bhattacharya and D. Divan, "Synchronous frame based controller implementation for a hybrid series active filter system," in *Proc. 13th Ind. Appl. Soc. Annu. Meeting*, 1995, pp. 2531–2540.

[10] K. Chatterjee, B. G. Fernandes, and G. K. Dubey, "An instantaneous reactive volt-ampere compensator and harmonic suppressor system," *IEEE Trans. Power Electron.*, vol. 14, no. 2, pp. 381–392, Mar. 1999.

[11] V. B. Bhavaraju and P. N. Enjeti, "Analysis and design of an active power filter for balancing unbalanced loads," *IEEE Trans. Power Electron.*, vol. 8, no. 4, pp. 640–647, Oct. 1993.

[12] H. Abaali *et al.*, "Shunt active power filter control under non-ideal voltage conditions," *Int. J. Inf. Technol.*, vol. 2, no. 2, pp. 164–169, 2005.

[13] S. P. Dubey, P. Singh, and H. V. Manjunath, "DSP based neural network controlled parallel hybrid active power filter," *Int. J. Emerging Elect. Power Syst.*, vol. 4, no. 2, 2005, Article 2.

[14] B. N. Singh *et al.*, "Design and digital implementation of active filter with power balance theory," in *Proc. IEEE EPA*, Sept. 2005, vol. 2, no. 5, pp. 1149–1160.

[15] G. Bhuvaneswari and M. G. Nair, "A novel current compensation technique for shunt active power filters," in *Proc. IASTED Conf. Power Energy Systems*, 2003, pp. 109–113.

[16] R. A. Gayakwad, *Op-Amps and Linear Integrated Circuits*, 3rd ed. New Delhi, India: Prentice Hall India, 1993.

[17] P. Singh, Pacas, and C. M. Bhatia, "A new control scheme for harmonic and reactive power compensation in three-phase power systems," presented at the PCIM, Nurnberg, Germany, Jun. 2000.

[18] G. Bhuvaneswari and M. G. Nair, "A novel current compensation algorithm for a three-phase system feeding non-linear and reactive loads," in *Proc. IEEE IAS Int. Conf. Petroleum Chemical Industries*, New Delhi, India, Nov. 9–10, 2004, pp. 50–54.

G. Bhuvaneswari (SM'99) received the M.Sc. and Ph.D. degrees from the Department of Electrical Engineering, Indian Institute of Technology (IIT), Madras, India.

She was a Faculty Member with Anna University, Madras, for about two years and then was with the electrical utility ComEd, Chicago, IL. Since 1997, she has been a faculty member in the Department of Electrical Engineering, IIT, Delhi where she is an Associate Professor. Her areas of interest are power electronics, electrical machines, drives, and power quality.

Dr. Bhuvaneswari is a Life Fellow of the Institution of Electronics and Telecommunication Engineers (IETE).

Manjula G. Nair received the Ph.D. degree from Indian Institute of Technology, Delhi.

Currently, she is with the Department of Electrical Engineering, Amrita School of Engineering, Tamilnadu, India. Her areas of interest are fuzzy and ANN-based control of power systems and power quality.